Influence of tip-surface interactions and surface defects on Si(100) surface structures by low-temperature (5 K) scanning tunneling microscopy

D. Riedel, M. Lastapis, M. G. Martin, and G. Dujardin

Laboratoire de Photophysique Moléculaire, Bât. 210, Université Paris Sud, 91405 Orsay, France

The Si(100) surface structures on n-type degenerately doped samples ($\rho \sim 0.005~\Omega$ cm) have been investigated with a scanning tunneling microscope (STM) at very low temperature (~ 5 K). We have developed a method to monitor quantitatively the proportion of the various observed surface structures [$p(2\times2)$, $c(4\times2)$ and flickering]. This study has been performed as a function of the tunnel current and the presence (or not) of surface defects in the observed areas. The *normal* surface areas having a low density of defects ($\sim 1\%$) have been observed to vary from the $p(2\times2)$ to the $c(4\times2)$ structures when the tunnel current increases. This indicates that the STM tip-surface interaction strongly influences the observed structures. Furthermore, surface areas completely *free* of any defects are dominated by flickering structures.

Over the past 20 years, the atomic structure of the Si(100) reconstructed surface has been the subject of intense experimental and theoretical work. The first low-temperature scanning tunneling microscope (STM) experiment at 120 K by Wolkow[1] nicely confirmed that the flip-flop motion of the Si dimers which occurs at room temperature is frozen at this temperature giving rise to a $c(4\times2)$ reconstruction. It was expected that the $c(4\times2)$ structure would remain the most stable structure down to very low temperature. However, quite surprisingly, recent STM experiments have shown that new reconstructions such as symmetric dimers[2–3] or static $p(2\times2)$ structures[4] can be observed at very low temperature (<10 K). There have been several controversial discussions concerning the origin of these new reconstructions.[3–6] Very recently, Sagisaka *et al.*[6] suggested that the scattered electrons issued from the STM tip might be responsible for the observed transition from the $c(4\times2)$ to the $p(2\times2)$ reconstruction.[7] This structure manipulation has been evidenced by plotting the evolution of the STM topographies as a function of the surface voltage and tunnel current. Nevertheless, we have observed that such surface structure modifications occur when the imaging of the same area is repeated even though the surface voltage and tunnel current are kept constant. Under such conditions, it is difficult to demonstrate the influence of the STM tip interaction with the surface, only by showing various images recorded at different surface voltages and tunnel currents. In this paper, we propose a statistical approach to clarify this structure manipulation with the STM tip. The Si(100) (n-type, As doped) surface after cooling down to 5 K has been observed under a positive and negative surface voltage. For the positive surface voltage, we have counted the proportion of silicon dimers observed in a $c(4\times2)$, $p(2\times2)$ or flickering surface structure relative to the total number of dimers observed in the scanned area. By plotting this proportion of each of these structures (structure probability) as a function of the tunnel current, we find that the $p(2\times2)$ structure shows a strong tendency to be transformed into the $c(4\times2)$ structure when the STM tip surface interaction increases on *normal* surface areas (defects $<1\%$). Furthermore, we demonstrate that the flickering structure

dominates the surface areas that are completely *free* of defects. The influence of these two effects; the STM-tip surface interaction and surface defects, makes the study of this surface reconstruction a very difficult task.

The experiments have been performed with an ultrahigh vacuum (UHV) low-temperature (LT) scanning tunneling microscope (STM).[8] It is composed of a load-lock chamber, a preparation chamber, and a STM chamber. The STM UHV chamber is equipped with a four-liter liquid helium cryostat bath to which the whole STM is connected. This ''*beetle*'' type[9] STM is surrounded with a double radiation shield inside the STM chamber. The external shield is cooled with a liquid nitrogen bath while the internal shield is cooled with the liquid helium bath. The shields are pierced on the sides with removable windows or shutters permitting different functionalities: observation, laser irradiation, or molecular deposition. A front shutter permits samples and tips to be transferred via a cooled manipulator from the preparation chamber. The temperature inside the STM is measured at two points with two silicon diodes (DT-470, Lake shore). The temperatures indicated in this paper correspond to the temperature of the base plate of the STM situated near the sample holder. It indicates the temperature of the sample, after stabilization of the cooling process, with a precision of ± 0.25 K in the range 2–100 K. The preparation chamber can receive samples or tips from the load-lock chamber and is equipped with a thermal sensor on its manipulator and electrical connection to sample holders or tip holders. The samples used in this experiment are prepared in an ultrahigh vacuum chamber with a base pressure of 7×10^{-11} Torr. They are Si(100) n-type As doped with a resistivity $\rho \sim 0.004 - 0.006~\Omega$ cm and a thickness $e \sim 100~\mu$m. The preparation of the silicon sample starts by resistively heating to $650\,°$C for a predegassing period of about 12 h. The sample holder is then cooled to ~ 6 K with a liquid He circulation through the manipulator while the heating of the sample is kept fixed. We then proceed to rapidly flash the sample as explained in other works,[10] with a slow decline in temperature from 950 to $750\,°$C. The sample is then cooled back down to 6 K and transferred into the STM chamber at this temperature. This procedure allows us to obtain very
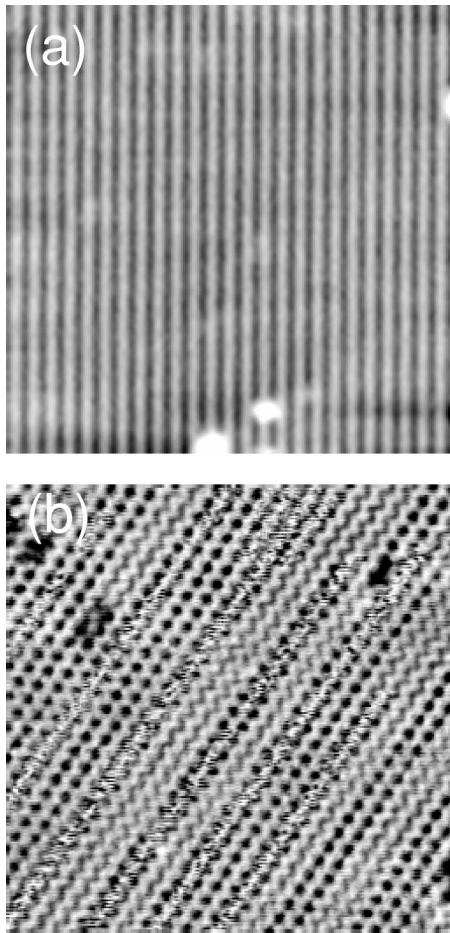
FIG. 1. Si(100) STM topographies from *n*-type samples acquired at 5 K. (a) 18×18 nm^2, $V_s = -1.5$ V, and $I = 0.56$ nA. (b) 16×16 nm^2, $V_s = +1.0$ V, and $I = 0.56$ nA with a rotation angle of 45°. Mixture of $p(2 \times 2)$, $c(4 \times 2)$ and flickering dimers.
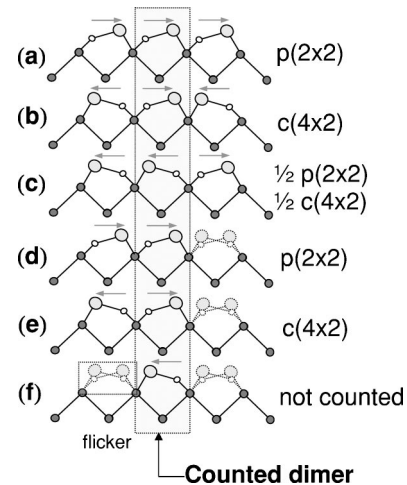

FIG. 2. Schematics of the categorizing method of individual silicon dimers involved in specific structures. (a), (b) Dimer in a "pure" $c(4 \times 2)$ or $p(2 \times 2)$ structure, respectively. (c)–(e) Dimers in partial structures. (f) Not counted dimer.

clean sample surface reconstructions with a mean value of the defect density[11] smaller than 1%.

In order to avoid any artifact due to the sample or the STM tip, the experiments have been repeated with three different samples (all *n*-type) and three different tips. Similarly to what has been observed in previous studies,[4] the STM topographies show a clear $p(2 \times 1)$ symmetric reconstruction when recorded at negative surface voltages [Fig. 1(a)] whereas they show a mixture of $c(4 \times 2)$, $p(2 \times 2)$ and flicker structures when recorded at a surface voltage of $+1.0$ V [see Fig. 1(b)]. We emphasize here that the STM topography shown in Fig. 1(b) is continuously changing when the imaging of the same surface area is repeated while the tunneling parameters (surface voltage and tunnel current) remain the same. In particular, the proportion of silicon dimers involved in each structure [$c(4 \times 2)$, $p(2 \times 2)$ and flickering] is continuously changing between two STM images (i.e., the proportion of dimers involved in a structure can vary by up to 50% from one STM topography to another). Under such conditions, it is impossible to investigate the surface structure modifications as a function of the tunnel current from the sole qualitative observation of the STM topographies as it has been done in previous studies.[2–6] In

this paper, we have developed a method to evaluate quantitatively, the proportion of each surface structure [$c(4 \times 2)$, $p(2 \times 2)$ and flickering]. The method consists in counting all the individual dimers on each STM image and to classify them in three categories depending on which structure the dimer is involved in (see Fig. 2). The probability of each structure is obtained by dividing the corresponding number of silicon dimers by the total number of silicon dimers in the whole STM image. The obtained probabilities are then averaged over three to ten STM images acquired with the same surface voltage and the same tunnel current ($\sim 16 \times 16$ nm^2 image size). Each silicon dimer is categorized by taking into account its position (i.e., antiferromagnetic or ferromagnetic) relative to the position of the nearest neighbor dimer in the dimer row to the left and to the right. The position of the dimer situated *above* or *below* the counted dimer within the same dimer row is, for the most part, observed as a buckled dimer as has been predicted theoretically.[12] Therefore the categorization method does not take directly into account these two dimers (*above* or *below*) unless they are not buckled with respect the counted dimer (e.g., a dimer that is next to a defect in the same row or a discontinuity in the buckling along the dimer row). In such cases, the considered dimer is not counted. As shown in Fig. 2, we have defined several situations. (i) A dimer involved in a *pure* $c(4 \times 2)$ [or $p(2 \times 2)$] structure [Figs. 2(a) and 2(b), respectively] implies that its nearest neighbors to its left and to its right have to be antiferromagnetic (ferromagnetic), respectively. (ii) Other configurations shown in Figs. 2(c)–2(e) count dimers in the following partial structure categories: $\frac{1}{2}p(2 \times 2) + \frac{1}{2}c(4 \times 2)$, $p(2 \times 2)$, $c(4 \times 2)$, respectively. (iii) Additionally, a buckled silicon dimer, surrounded by two dimers that do not form a partial or a *pure* structure [Fig. 2(f)] is not counted in the statistics. Therefore, the structure probabilities noted $c(4 \times 2)^*$, $p(2 \times 2)^*$ and *flicker* are calculated from the sum of all dimers counted in each structure category described in Fig. 2. For a surface voltage of $V_s = +1.0$ V we have plotted in Fig. 3 the probabilities of the $c(4 \times 2)^*$, $p(2 \times 2)^*$ and
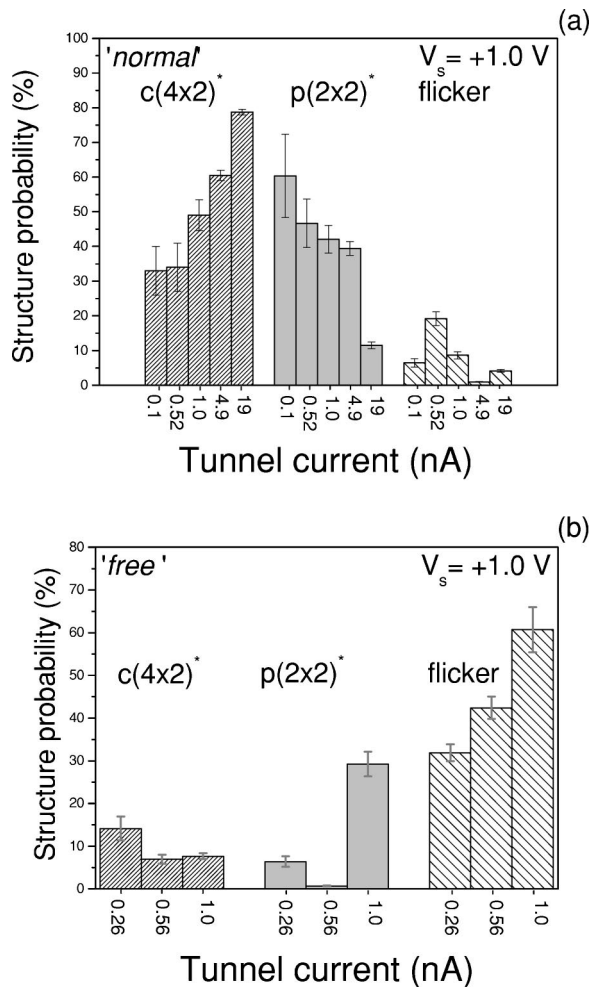
FIG. 3. Histograms of the probability of three different structures distinguished on the surface. (a) Probability of the $c(4 \times 2)^*$, $p(2 \times 2)^*$ and flickering structures for a constant positive surface voltage of $V_s = +1.0$ V and for tunnel currents from 0.1 to 19 nA. The scanned areas are ''normal'' (with less than 1% of defects). (b) The same as (a) but for areas ''free'' of defects and for tunnel currents from 0.26 to 1 nA. Error bars (standard error in the mean) are indicated.

flicker structures for tunnel current values varying from 0.1 to 19 nA. We have made a distinction between the results obtained from surface areas which are completely *free* of any defects, i.e., surface areas which have no defects within a distance of 20 nm at least [Fig. 3(b)] and *normal* surface areas. We emphasize that the *normal* surface areas whose structure may be influenced by defects have nevertheless a very low concentration of defects ($<1\%$) [Fig. 3(a)].

Let us first discuss the results for the normal surface areas. It is clear from Fig. 3(a), that at $V_s = +1.0$ V the proportion of the $c(4 \times 2)$ structure increases as the tunnel current increases from 0.5 to 19 nA. This correlates directly with the proportion of $p(2 \times 2)$ structure which decreases as the tunnel current increases from 0.5 to 19 nA. As a result, the surface is almost completely $c(4 \times 2)$ for a tunnel current of 19 nA [Fig. 4(a)]. It is striking to note that similar results have been mentioned by Sagisaka *et al.*,[6] however, for tunnel currents three orders of magnitude smaller than in our case.
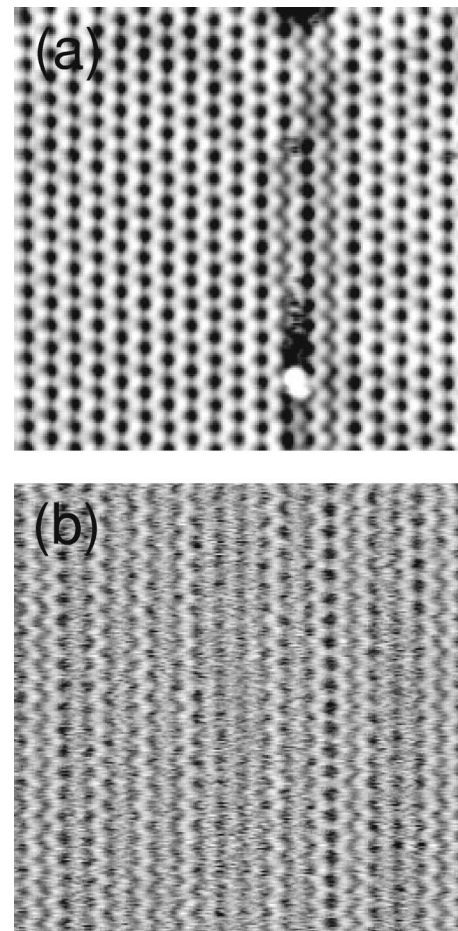

FIG. 4. Si(100) STM topographies from *n*-type samples acquired at 5 K. (a) 14×14 nm^2, $V = +1.0$ V, and $I = 19$ nA. The defect zone is mainly surrounded by the $p(2 \times 2)$ structure while the rest ($\sim 80\%$) of the scanned area is composed of a $c(4 \times 2)$ structure. (b) 15×15 nm, $V = +1.0$ V, and $I = 0.56$ nA. The scanned area is defect free and composed mainly of flickering dimers ($\sim 50\%$).

Indeed, Sagisaka *et al.*[6] observed at $V_s = +1.3$ V a transition from a $c(4 \times 2)$ to a $p(2 \times 2)$ when decreasing the tunnel current from 30 to 5 pA whereas we have observed a similar effect at $V_s = +1.0$ V when decreasing the current from 19 to 0.52 nA. This discrepancy may be explained by a higher density of defects and/or from a lack of quantitative measurements in Ref. 6. Our results on *normal* surface areas indicate that for a high STM tip-surface interaction (high tunnel current), the surface tends to be dominated by the $c(4 \times 2)$ structure whereas for a weaker tunnel current interaction (low tunnel current) the $p(2 \times 2)$ structure dominates. It is not possible to specify here what kind of STM tip-surface interaction is the most effective since all kinds of interactions are expected to increase when the tunnel current increases (i.e., the electric field effect,[13] the inelastic electron effect,[14,15] the direct tip-surface contact[16,17]).

We will now discuss the structure of surface areas *free* of defects [see Fig. 3(b)]. The role of surface defects is important and has never been properly evaluated. Indeed, it seems that the surface defects play a role in the surface reconstruc-

tion even if they are located 10–20 nm away from the observed surface area. Results in Fig. 3(b) indicate that the *free* areas are dominated by the flickering structure as shown in Fig. 4(b). This structure consists in unstable silicon dimers which have a "slow" flip-flop motion when the STM tip passes over the dimers. This finding that the flicker structure dominates in the defect free surface areas, provides a possible reconciliation with previous works which were in apparent contradiction. For example, the observation of an almost complete flickering structure at a surface voltage of +1.0 V by Yokoyama *et al.*[2] might be explained by a very low density of defects. On the contrary, the observation of $c(4\times2)$ and $p(2\times2)$ structures at the same surface voltage by other authors[3,6] might be explained by the presence of surface defects, even at a relative low density.

In conclusion, we have proposed a method to quantitatively monitor the various structures of the Si(100) surface observed at low temperature (5 K) with an STM. We have found that at a surface voltage of +1.0 V, the observed surface structures are different depending on whether it is ob-served on *normal* surface areas which contain a low density of defects (<1%) or on *free* surface areas which are completely free of any defects. On the *normal* surface areas, STM tip-surface interactions, able to modify the surface structures, have been evidenced by varying the tunnel current. At $V_s = +1.0$ V, an increase in the tunnel current, i.e., the increase of STM tip-surface interaction, favors the $c(4\times2)$ structure to the detriment of the $p(2\times2)$ and flickering structures. We have also found that on the *free* surface areas imaged at $V_s = +1.0$ V, the flicker dimers dominate the surface structure. These results illustrate the extreme complexity of the Si(100) surface reconstruction studies at 5 K. Indeed both the STM tip-surface interactions and the influence of surface defects (even when located relatively far away from the studied surface area) need to be properly taken into account for a complete understanding of this surface reconstruction.

[1] R. A. Wolkow, Phys. Rev. Lett. **68**, 2636 (1992).

[2] T. Yokoyama and K. Takayanagi, Phys. Rev. B **61**, R5078 (2000).

[3] K. Hata, S. Yosnida, and H. Shigekawa, Phys. Rev. Lett. **89**, 286104 (2002).

[4] Y. Kondo, T. Amakusa, M. Iwatsuki, and H. Tokumoto, Surf. Sci. **453**, L318 (2000).

[5] T. Mitsui, K. Takayanagi, Phys. Rev. B **62**, R16 251 (2000).

[6] K. Sagisaka, D. Fujita, and G. Kido, Phys. Rev. Lett. **91**, 146103 (2003).

[7] W. A. Hofer, A. J. Fisher, R. A. Wolkow, and P. Grütter, Phys. Rev. Lett. **87**, 236104 (2001).

[8] F. Moresco, G. Meyer, H. Tang, C. Joachim, and K. H. Rieder, J. Electron Spectrosc. Relat. Phenom. **129**, 149 (2003).

[9] G. Meyer, Rev. Sci. Instrum. **67**, 2960 (1996).

[10] K. Hata, T. Kimura, S. Ozana, and H. Shigekawa, J. Vac. Sci. Technol. A **18**, 1933 (2000).

[11] Defect density is measured from several images and corresponds to the ratio of the defects number (i.e., missing dimers number, type *c* defects, or impurities counted as hidden dimers) to the total number of dimers observed in the scanned area.

[12] S. B. Healy, C. Filippi, P. Kratzer, E. Penev, and M. Scheffler, Phys. Rev. Lett. **87**, 016105 (2001).

[13] P. A. Sloan, M. F. G. Hedouin, R. E. Palmer, and M. Persson, Phys. Rev. Lett. **91**, 118301 (2003).

[14] J. I. Pascual, N. Lorente, Z. Song, H. Conrad, and H.-P. Rust, Nature (London) **423**, 525 (2003).

[15] L. J. Lauhon and W. Ho, Surf. Sci. **451**, 219 (2000).

[16] L. Bartels, G. Meyer, and K.-H. Rieder, Phys. Rev. Lett. **79**, 697 (1997).

[17] G. Dujardin, A. J. Mayne, O. Robert, F. Rose, C. Joachim, and H. Tang, Phys. Rev. Lett. **80**, 3085 (1998).